GCAGS JOURNAL
A Publication of the Gulf Coast Association of Geological Societies
www.gcags.org

Organic-Matter Pores: New Findings from Lower-Thermal-Maturity Mudrocks

Robert M. Reed

Bureau of Economic Geology, Jackson School of Geosciences, University of Texas at Austin, University Station, Box X, Austin, Texas 78713–8924, U.S.A.

ABSTRACT

New pore analyses of low-thermal-maturity (R_o <0.7%) organic matter of possible or probable terrestrial origin (type III kerogen) from three mudrock units in Texas contradict previous pore work on low-thermal-maturity, mostly marine organic matter from the Barnett and Eagle Ford Shales. In early work on mudrocks containing primarily marine organic matter, organic matter at R_o <0.75% was observed to typically lack pores, whereas some thermally mature organic matter did develop pores. However, this pattern of pore development was not observed by all researchers working on other units, some of whom did see pores in organic matter at lower thermal maturities. To understand if predepositional pores in terrestrial organic matter are responsible for the discrepancy in pattern, this study focuses on organic matter at low thermal maturities, which should not have thermally generated pores.

Two beds of organic-matter-rich mudrock from a terrestrial depositional environment were sampled from the Paleogene Wilcox Group of East Texas. The mudrocks have an R_o of <0.5%, a siliceous–argillaceous composition, and >11% total organic carbon (TOC). Based on Rock-Eval pyrolysis results and depositional setting, the kerogen is thought to be dominantly type III. Some silt-size organic-matter grains in these samples contain probable predepositional pores. Pore sizes are up to 5 µm in length, and up to 27% of the organic matter has pores. Pores are more common in the larger organic-matter grains.

Samples from one core interval of the basal Cretaceous Eagle Ford Group on the San Marcos Arch of South Texas have abundant vitrinite (R_o ~0.45%) based on visual analysis, in contrast with shallower layers, which are vitrinite-poor. Rock-Eval pyrolysis results suggest the presence of type III kerogen. Although these basal mudrock samples are more argillaceous than the rest of the Eagle Ford, they were deposited in a marine environment. Some of the organic matter in these samples has predepositional pores. Some of these pores are elongate, with sizes >1 µm.

Pennsylvanian Smithwick Shale samples from the Fort Worth Basin of Texas have thermal maturity ranging from 0.4 to 0.71% Ro. Although much of the unit is marine, observed plant fossils suggest a mixed-organic-matter source. Some Rock-Eval pyrolysis results also suggest type III kerogen. Much of the organic-matter shows a newly identified organic-matter pore texture. Instead of consisting of a mass of organic matter with spherical holes, the organic-matter is a composite grain made up of smaller, spherical organic-matter bodies. These organic-matter bodies vary slightly in size, but most are 60 to 100 nm in diameter. Pore space is present between the organic-matter bodies. Several possible formation mechanisms exist for these organic-matter bodies, but they strongly resemble "nannobacteria" described by previous researchers.

INTRODUCTION

Pores in organic matter present in mudrocks have proven to be important for production of hydrocarbons from these formations (e.g., Loucks et al., 2009, 2012; Curtis et al., 2010; Schieber, 2010; Klaver et al., 2012, 2015; Cardott et al., 2015). Some early work on organic-matter pores found in mudrocks focused on the Barnett Shale (Loucks et al., 2009) and the Eagle Ford Group (e.g., Reed and Ruppel, 2012; Pommer and Milliken, 2015). In these rocks with organic matter of primarily marine origin (Pollastro et al., 2007; Pommer and Milliken, 2015), a pattern of organic-matter pore development was recognized. At vitrinite reflectances (R_o) less than 0.75%, organic matter was typically without pores (Loucks et al., 2009; Reed and Ruppel, 2012), whereas more-thermally-mature organic matter tended to develop pores. This pattern of pore development was not necessarily observed by researchers working on other units such as the Kimmeridge Clay (Fishman et al., 2012) or Mediterranean marine sapropels (Milliken et al., 2014). Those studies found some pores in organic matter at low to very low thermal maturities. In order to better understand this discrepancy and if these pores could be predepositional, this study focuses on what are either known to be or are probably terrestrial organic-matter grains at low thermal maturities (<0.75% Ro). Thirteen samples were

Manuscript received March 15, 2017; revised manuscript received June 13, 2017; manuscript accepted July 5, 2017.

GCAGS Journal, v. 6 (2017), p. 99–110.

examined from three different units (Wilcox Group, Eagle Ford Group, and Smithwick Shale) from three areas in Texas (Fig. 1).

This study reports on micrometer- to nanometer-scale pores in discrete silt- to sand-size masses of organic matter. There is considerable difference in opinion over what to call these masses: grains, particles, or macerals. While acknowledging that most of them would be identified as macerals using optical petrology, using SEM imaging identification of maceral type is difficult at best. I have chosen to refer to them as "grains" to emphasize the pieces are primarily thought to have been transported, rather than forming in situ or falling from suspension.

METHODS

Most samples were sent to GeoMark Research for Rock-Eval pyrolysis and LECO TOC measurements (Table 1). Rock-Eval T_{max} values were converted to calculated R_o values using the formula of Jarvie et al. (2001). In one core from the Eagle Ford

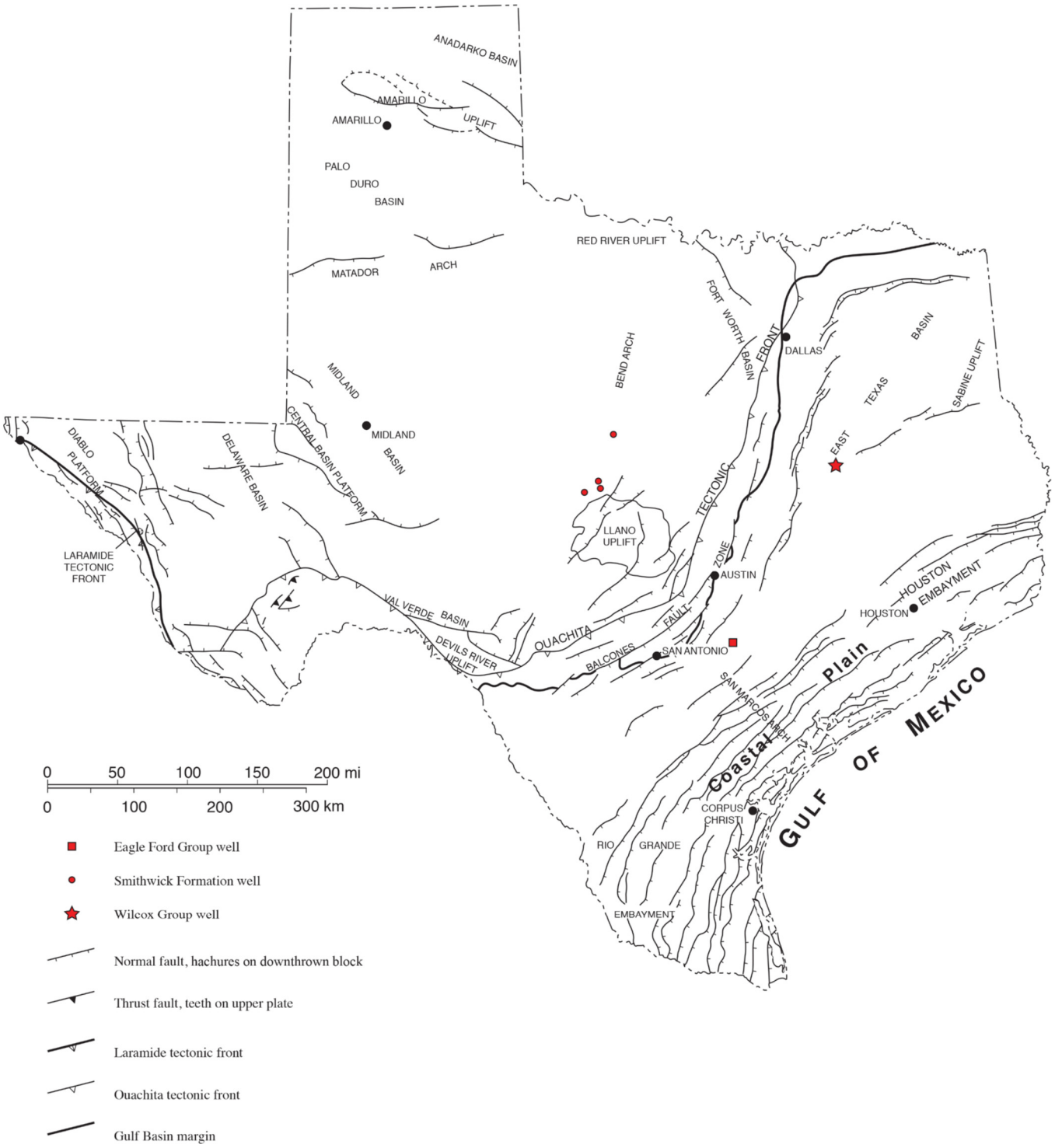

Figure 1. Map of Texas showing location of sampled wells and major tectonic features (modified after Bureau of Economic Geology, 1997).

Well Name	County	Depth (ft)	Unit Name	LECO TOC	S1	S2	S3	T_{max} (°C)	Calc. % R_o	Meas. % R_o	HI	OI	S2/S3	S1/TOC	PI
LN–2C–82 A–00412	Leon	192	Wilcox	14.4	2.39	0.44	7.17	425	0.49	0.3	156	50	3	17	0.1
LN–2C–82 A–00412	Leon	199	Wilcox	11.3	2.07	25.08	4.91	426	0.51	0.32	222	43	5	18	0.08
C. J. Hendershot #1	Gonzales	4762.5	Eagle Ford	–	–	–	–	–	–	0.43	–	–	–	–	–
C. J. Hendershot #1	Gonzales	4771	Eagle Ford	8.29	2.87	65.37	0.83	426	0.51	0.48	789	10	79	35	0.04
C. J. Hendershot #1	Gonzales	4774	Eagle Ford	1.83	0.46	4.44	0.38	420	0.4	–	243	21	12	25	0.09
R. V. Neal A–1–1	McCulloch	147	Smithwick	6.11	0.2	5.31	1.14	422	0.44	–	87	19	5	3	0.04
C. D. Scoggins A–2–1	McCulloch	442	Smithwick	5.88	0.15	5.58	0.6	427	0.53	–	95	10	9	3	0.03
H. G. Johanson MC–1	McCulloch	901	Smithwick	6.65	0.46	13.23	0.6	434	0.65	–	199	9	22	7	0.03
H. G. Johanson MC–1	McCulloch	908	Smithwick	5.38	0.22	6.56	0.35	436	0.69	–	122	7	19	4	0.03
J. A. Potter C–9–1	Brown	1930.7	Smithwick	0.44	0.05	0.17	1.13	0	–	–	38	255	0	11	0.23
J. A. Potter C–9–1	Brown	1943.1	Smithwick	2.06	0.25	1.82	0.67	435	0.67	–	88	33	3	12	0.12
J. A. Potter C–9–1	Brown	2007.5	Smithwick	4.6	0.82	4.93	0.36	434	0.65	–	107	8	14	18	0.14
J. A. Potter C–9–1	Brown	2065.6	Smithwick	2.02	0.29	1.59	0.21	437	0.71	–	79	10	8	14	0.15

Table 1. TOC and Rock-Eval data report. TOC = weight percent total organic carbon; S1, S2 = mg of hydrocarbons per gram of rock; S3 = mg of carbon dioxide per gram of rock; HI = hydrogen index, mg of hydrocarbon per gram TOC; OI = oxygen index, mg of carbon dioxide per gram TOC; and PI = production index. Vitrinite reflectance (R_o) calculated from T_{max} using the equation of Jarvie et al. (2001).

Group, measured vitrinite-reflectance data from an unpublished study by the USGS National Coal Resources Data System (J. C. Hower, 2017, personal communication) were available to supplement Rock-Eval data.

Samples were prepared for scanning electron microscope (SEM) examination using broad ion-beam (BIB) milling with Ar ions. Samples were processed using a Leica EM Triple Ion-Beam Cutter (TIC) 020 system. Samples were ion-milled using an accelerating voltage of 8 kV, a source current of 2.8 mA, and a milling time of 10 hr. Milled surfaces are perpendicular to bedding. All BIB samples were given an ~6 nm coating of Ir to prevent charge buildup during SEM examination. BIB samples were imaged using a field-emission SEM: an FEI Nova NanoSEM 430 model equipped with dual Bruker XFlash® SDD energy dispersive spectroscopy (EDS) systems for element identification and mapping. Moderate accelerating voltages (10–15 kV) were used on these systems to avoid causing electron-beam damage to the samples. SEM working distances for secondary electron (SE) and backscattered electron (BSE) imaging were ~6 mm; for EDS mapping, 9 to 10 mm. Both SEM images and EDS element maps were collected from all samples. Point counting and measurements of grains and pores in SEM images were done using JMicroVision software (Roduit, 2008).

SAMPLES, THERMAL MATURITY, AND KEROGEN TYPE

Wilcox Group

The Paleogene (Paleocene-Eocene) Wilcox Group of East Texas contains both terrestrial and shallow-marine clastic sedimentary rocks (e.g., Fisher and McGowen, 1969). The unit is located above the Midway Group and below the Claiborne Group. One very shallow core from Leon County in East Texas (Fig. 1) was sampled (Bureau of Economic Geology–TENRAC borehole LN–2C–83). The core has been assigned to the upper Calvert Bluff Formation in the upper part of the Wilcox Group (Mukhopadhyay, 1989). The core contains two ~1 ft (~0.305 m) layers of organic-rich argillaceous mudrock sandwiched between thin layers of fine to very fine sandstone. The sequence is interpreted to be from a floodplain setting (W. A. Ambrose, 2016, personal communication). Both of the mudrock layers were sampled for Ar–ion milling and SEM examination. Sample depths were 192 and 199 ft (58.5 and 60.4 m). Samples are from same layers as samples #51 and #52 from Mukhopadhyay (1989).

The organic-rich Wilcox Group mudrocks from the sampled core are at a relatively low thermal maturity. Mukhopadhyay (1989, his samples 51 and 52) reported huminite (a vitrinite precursor) reflectances of 0.30% and 0.32% for samples from the same organic-rich layers. The two samples from this study have calculated R_o values of 0.49% and 0.51% (Table 1) and TOC values of 11.30 wt% and 14.40 wt% (Table 1), respectively.

Two factors argue for a terrestrial origin of this Wilcox organic matter. Plots of Rock-Eval pyrolysis results (Figs. 2 and 3) suggest the presence of type III kerogen. The interpretation of the depositional environment as being a floodplain also calls for terrestrial kerogen. Mukhopadhyay (1989) showed that the samples were mostly huminites (proto-vitrinite) but also contained significant liptinites and inertinites.

Basal Eagle Ford Group

The Cretaceous Eagle Ford Group is a mostly calcareous mudrock unit present in the subsurface in South and East Texas (e.g., Hentz et al., 2014; Breyer, 2016). Samples for this study are from the basal section of the lower Eagle Ford Group just above the Cretaceous Buda Limestone. Samples were taken from the Tesoro C. J. Hendershot #1 core in Gonzales County, Texas, on the San Marcos Arch (Fig. 1). Harbor (2011) noted an increase in argillaceous material in the basal section and an argillaceous layer with a thickness of about 1 ft at the bottom of the section just above the Buda Limestone. Four samples were milled from three depths (4762.5, 4771, and 4774 ft [1451.6, 1454.2, and 1455.1 m]) in this lower part of the Eagle Ford section. Several other Eagle Ford samples from a previous pore study (Reed and Ruppel, 2012) were available from shallower depths in this core (4734 to 4758 ft [1442.9 to 1450.2 m]) for comparison of pore development and lithology.

The organic-matter makeup of the basal part of the Eagle Ford core is complicated. Previous work (J. C. Hower, 2017, personal communication) noted that samples studied from lower in the core (4762.5 ft and 4771 ft [1451.6 m and 1454.2 m]) have abundant vitrinite macerals. This is in contrast with shallower layers from the same well, which are vitrinite-poor despite being organic-rich (J. C. Hower, 2017, personal communication). Vitrinite reflectances from the lower samples were 0.43% and 0.48%, respectively (J. C. Hower, 2017, personal communication). Rock-Eval pyrolysis results of a sample from an argillaceous layer in the basal section (4774 ft [1455.1 m]) showed possible type III kerogen on one plot (Fig. 3) and a more-marine signature on another (Fig. 2). This sample has a calculated R_o of 0.4% and a TOC of 1.83 wt% (Table 1). Rock-Eval pyrolysis results (Table 1) of the vitrinite-bearing sample from 4771 ft (1454.2 m) gave a more-marine signature (Figs. 2 and 3) typical of the Eagle Ford and a higher TOC of 8.29 wt%. However, overall evidence suggests the basal section is enriched in terrestrial kerogen relative to the rest of the core.

Smithwick Shale

The Pennsylvanian Smithwick Shale occurs in the southern half of the Fort Worth Basin in north-central Texas (Kier et al., 1980), above the Mississippian Barnett Shale and below the Pennsylvanian Atoka and Strawn formations. This thick argillaceous unit is partly contemporaneous with and partly younger than the more calcareous Marble Falls Limestone (Kier et al., 1980). A number of cores from shallow wells drilled by Houston Oil and Minerals were available for this study (Fig. 1). Three sampled wells (H. G. Johanson MC–1, C. D. Scoggins A–2–1, R. V. Neal A–1–1) are in McCulloch County, Texas, and one (J. A. Potter C–9–1) is in Brown County, Texas. Nine Ar–ion-milled samples of various depths from the four wells were examined using the SEM. Sample depths range from 147 ft (44.8 m) to 2065.6 ft (629.6 m).

The Smithwick Shale samples have low thermal maturity, with variation between wells giving a range from 0.44% to 0.71% calculated R_o (Table 1). Thermal maturity appears to roughly correlate with current burial depth. Much of the Smithwick is organic-matter-poor, but samples for the current study were generally chosen for higher TOC content. TOC content ranges from 0.44 wt% to 6.65 wt%, with an average of 4.14 wt% (Table 1).

Although much of the unit is considered marine (e.g., Hughes and Rowe, 2010), outcrops of the Smithwick Shale contain abundant transported land-plant fossils, suggesting a mixed source of organics. Some of the results from Rock-Eval pyrolysis suggest the presence of type III kerogen (Fig. 3). However, the pseudo–van Krevelen plot (Fig. 2) yields ambiguous results that are reminiscent of plots for much higher thermal-maturity samples.

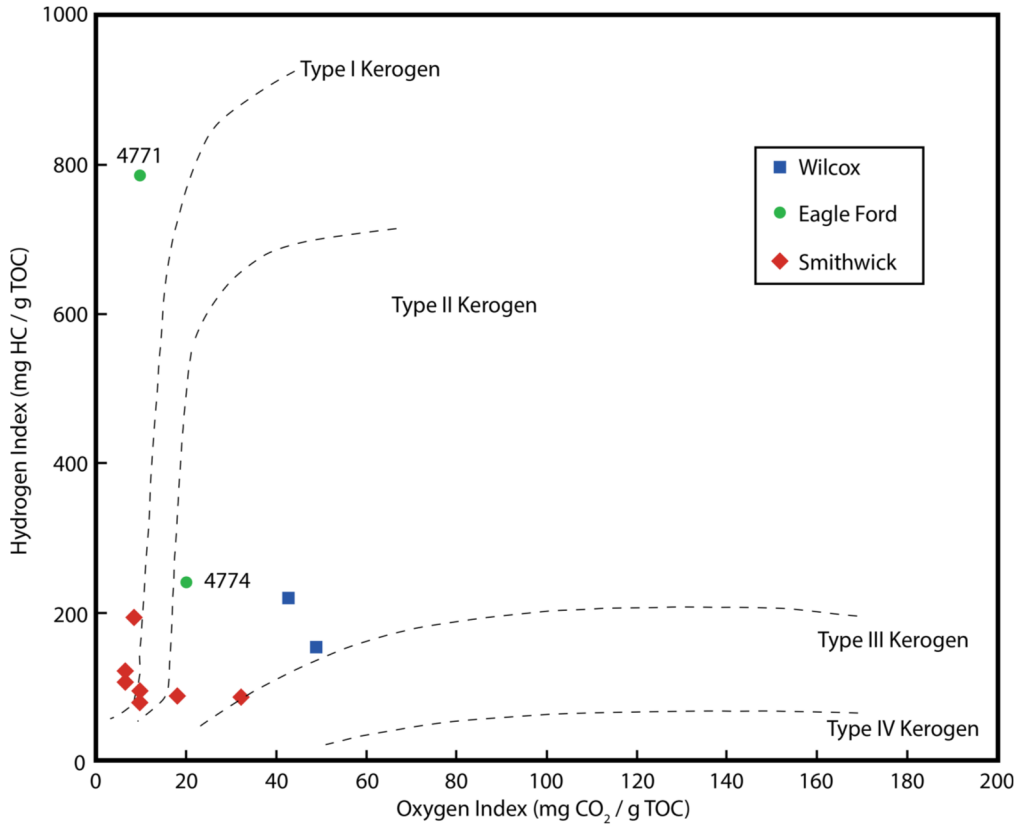

Figure 2. Pseudo–van Krevelen plot showing Rock-Eval data (HI versus OI) for the three different units. Wilcox Group samples are shown as squares, Eagle Ford Group samples as circles, and Smithwick Shale samples as diamonds.

SCANNING ELECTRON MICROSCOPE OBSERVATIONS

Wilcox Group

Overall composition of both of the Wilcox mudrock samples examined is siliceous-argillaceous with only minor calcite. Quartz grains are generally fine to very fine silt size but having a significant component of clay-size quartz, as well. Some silt-size mica grains are present. Mica and clay-mineral grains typically show alignment with bedding. One ion-milled sample contains a few sand-size euhedral crystals of gypsum that are concentrated in a small area.

Organic-matter grains are commonly silt-size particles. Some of the largest particles in the sample are the organic-matter grains. However, there is a wide range in particle size and shape, from very fine sand-size organic-matter grains to clay-size matrix organic matter. Many of the larger grains have rounded edges. Smaller organic-matter grains are generally more elongate and more ductile. The samples have a large number of interparticle pores between grains.

Some organic-matter grains in the Wilcox samples have pores. Pores seem more common in the larger organic-matter grains, although some of these are nonporous, as well. The smaller organic matter that occurs in the matrix is typically nonporous. Based on point counts of images, up to 27% of the organic matter in these samples is porous, although this varies from area to area.

Both the shapes of the pores in the organic-matter grains and the shapes of the grains themselves are heterogeneous. The multiple morphologies of organic-matter grains and pores suggest that several sources of porous organic matter contributed to these rocks. Some grains have cellular shapes (Figs. 4A and 4B) and are reminiscent of marine *Tasmanites* spores (e.g., Schieber, 1996) but smaller in size. The Wilcox grains also have pores in the organic matter that are not seen in *Tasmanites*. Other organic-matter grains are more equant (Figs. 4C and 4D). Pore arrangements vary from semipatterned (Fig. 4A) to more random (Fig. 4D). Wilcox organic-matter pore sizes, up to 5 µm in length (Fig. 4C), are generally larger than those formed through thermal maturation (e.g., Loucks et al., 2009; Milliken et al., 2013).

Basal Eagle Ford Group

Samples from three depths were Ar–ion milled and examined. The two shallower depths reported (J. C. Hower, 2017, personal communication) to have abundant vitrinite (4762.5 ft and 4771 ft [1451.6 m and 1454.2 m]) also had foraminifera and numerous coccolith fragments, indicating marine input. The overall composition is argillaceous–calcareous, with calcareous, coccolith-rich lenses (peloids) surrounded by more-argillaceous material. These samples have a few porous organic-matter grains. The porous organic-matter grains have few overall pores (Fig. 5A). Some samples from this core show textural evidence (organic-matter-filled foraminifera chambers) for some of the organic matter being migrated bitumen (Loucks and Reed, 2014; Milliken et al., 2014), despite the relatively low thermal maturity. Some migrated organic matter (bitumen) has a few micrometer-size pores relating to incomplete filling of intraparticle or interparticle pores (Ko et al., 2017b; Reed et al., 2017).

The basal sample from 4774 ft (1455.1 m), which has a type III kerogen chemical signature, is much different in all respects from the two shallower-depth samples. Lithologically the sample is clay-mineral-rich but also contains some very fine quartz silt and minor carbonate (Fig. 6). Some of the organic matter occurs in lenses mixed with clay-size mineral grains. Other organic matter occurs as discrete silt-size grains or clay-size matrix. A significant amount of the organic matter in this sample is porous (Figs. 5B–5D). Most pores are present in discrete grains of organic matter, although not all grains are porous. Some of this organic matter contains elongate pores greater than 1 µm in diameter (Fig. 5B). Other organic-matter grains have more-spherical pores with diameters less than 1 µm and smooth walls

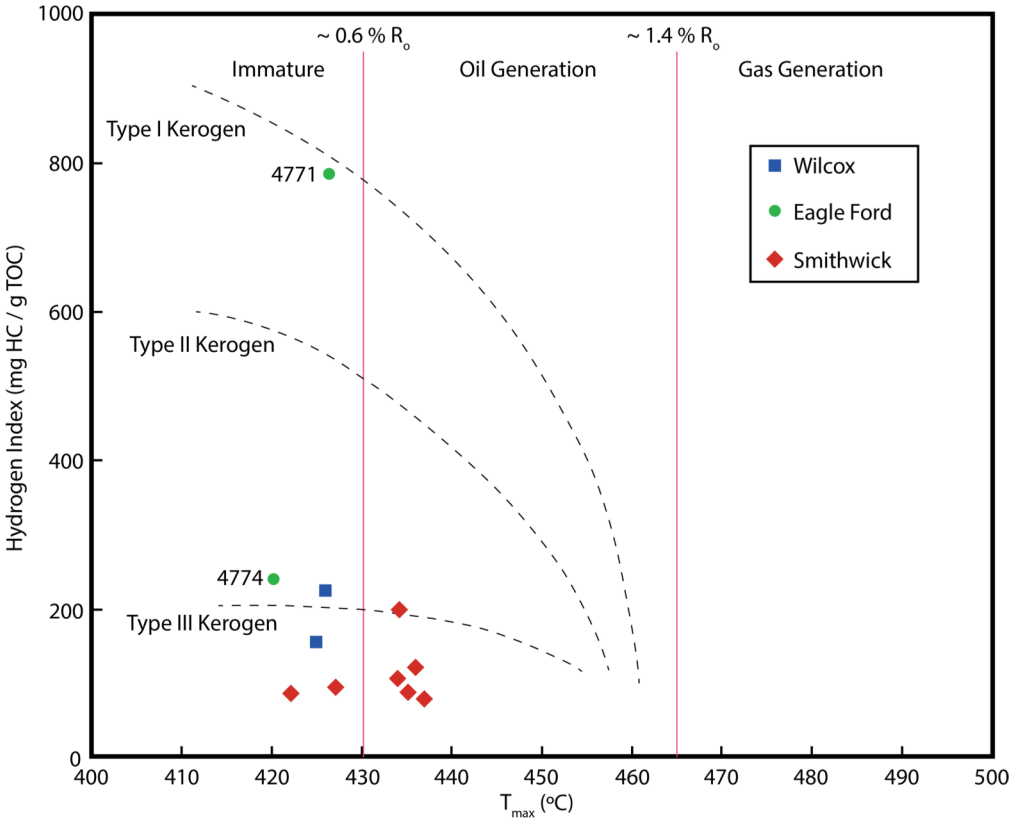

Figure 3. Graph showing Rock-Eval data (HI versus T_{max}) for the three different units. Wilcox Group samples are shown as squares, Eagle Ford Group samples as circles, and Smithwick Shale samples as diamonds.

(Figs. 5C and 5D). There is enough heterogeneity in pore morphology to indicate multiple sources of porous organic matter.

Smithwick Shale

Smithwick samples are typically siliceous–argillaceous mudrock, with varying but generally minor amounts of calcite. One sample has significant dolomite. Variable amounts of albite are present in the samples. Pyritized sponge spicules are prominent in two samples. Although there is variability in grain size, samples are relatively fine-grained even for mudrocks, with much of the material consisting of clay-size particles.

Organic matter in the Smithwick Shale is present both as discrete silt-size grains and as finer dispersed matrix material. Some of the organic-matter grains in the samples from the Smithwick Shale are nonporous; however, many organic-matter grains in almost all Smithwick samples show a distinct texture unlike that typically observed in other units. Instead of having the appearance of a solid mass of organic matter with spherical to elongate holes, as is common in many units (e.g., Barnett, Eagle Ford, Cline, and Haynesville), the Smithwick contains organic-matter grains that are a composite of smaller spherical organic-matter bodies (Fig. 7). These balls of organic matter are somewhat variable in size, but most are between 60 and 100 nm in diameter. Pore space is present between the organic-matter balls and bears a resemblance, at a much smaller scale, to the triangular-shaped interparticle pores common in sandstones. As thermal maturity and burial depth increase in the studied samples, based on visual estimates the intraparticle pore space in organic-matter grains decreases (Fig. 7D). Pore space diminishes, and the organic matter appears to be less spherical. Most of the porous organic-matter composite grains have lengths in the 5–10 µm

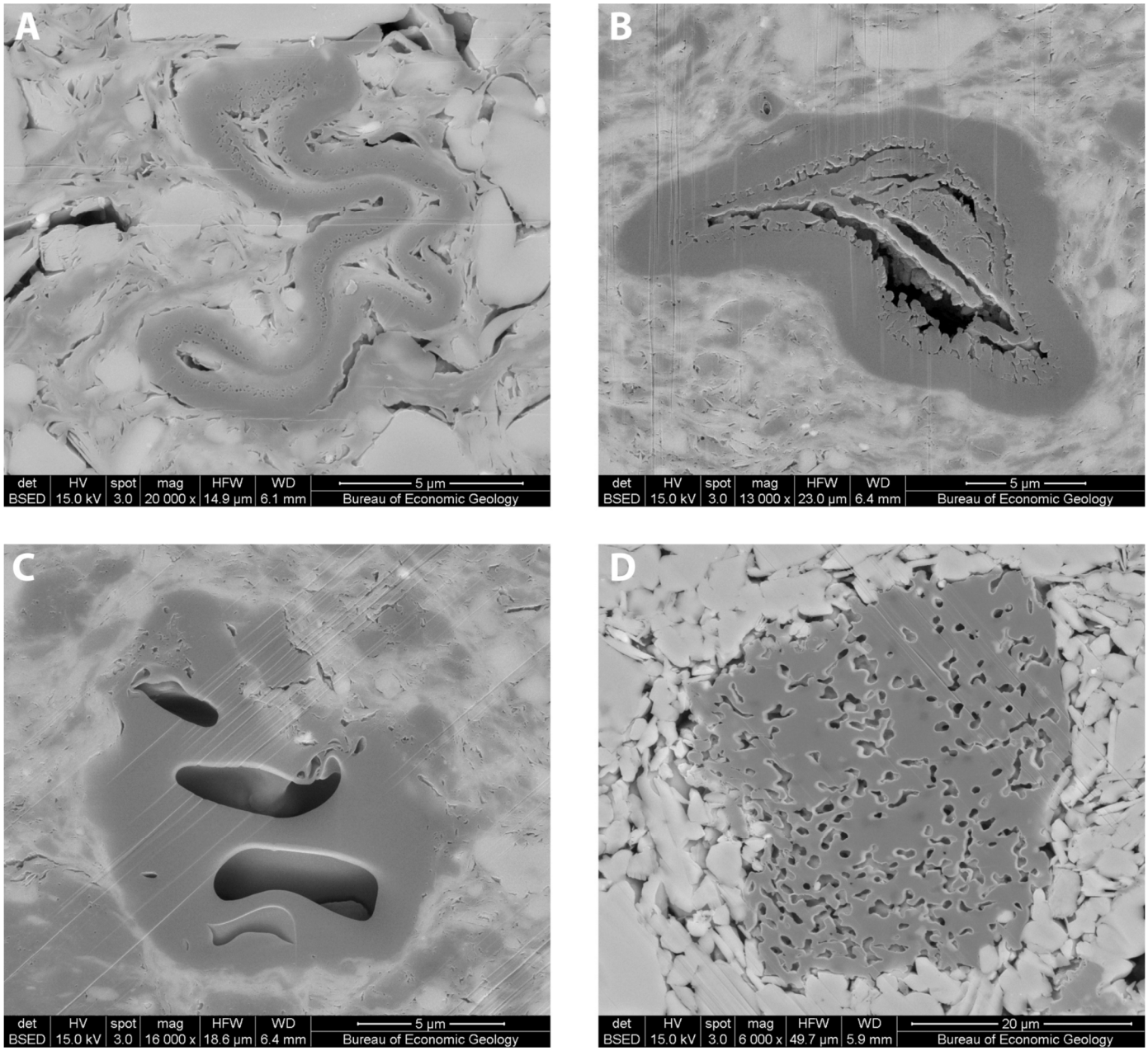

Figure 4. Backscattered electron (BSE) images of organic-matter grains with pores, Wilcox Group. (A) Complex spore-like organic-matter grain with small pores on the inner edge. (B) Organic-matter grain with a nonporous spore-like exterior and an extremely porous interior. (C) Organic-matter grain with a few large, rounded elongate pores. (D) Large organic-matter grain with large worm-like pores. Note abundance of interparticle pores outside this organic-matter grain.

range, although some composite grains up to 40 µm in length are present. Organic-matter composite grains are typically slightly elongate to elongate parallel to bedding. Rare organic-matter grains show more-spherical pores, similar to those seen in the Barnett Shale, though having developed at lower thermal maturities.

Since this strange porous texture was identified in the Smithwick samples, further imaging work has shown it is not unique to that unit. However, in organic-matter grains from other units, the texture is not widespread or even common. One composite grain showing this porous texture has been found in each of three different units: an organic-rich mudrock from the Paleogene Wilcox Group in East Texas, the Miocene Monterey Formation from California, and the Cretaceous Eagle Ford Shale of South Texas. All three of these composite grains are at R_o values less than 0.5%. One composite grain from the Mississippian Barnett Shale from North Texas also shows this texture, but at an R_o of ~1.0%. However, in these four composite grains the spheres of organic matter are larger, up to 500 nm in diameter.

DISCUSSION

Predepositional or Thermally Generated Pores?

There is some question about whether the organic-matter pores seen in these samples are predepositional or thermally generated. The presence of bitumen in the samples would indicate that thermal maturation—possibly enough to drive pore formation—had occurred. Lack of bitumen, on the other hand, would be one indicator that pores are predepositional. Tied to these observations is the further question of whether pore-containing organic matter is original kerogen or bitumen derived

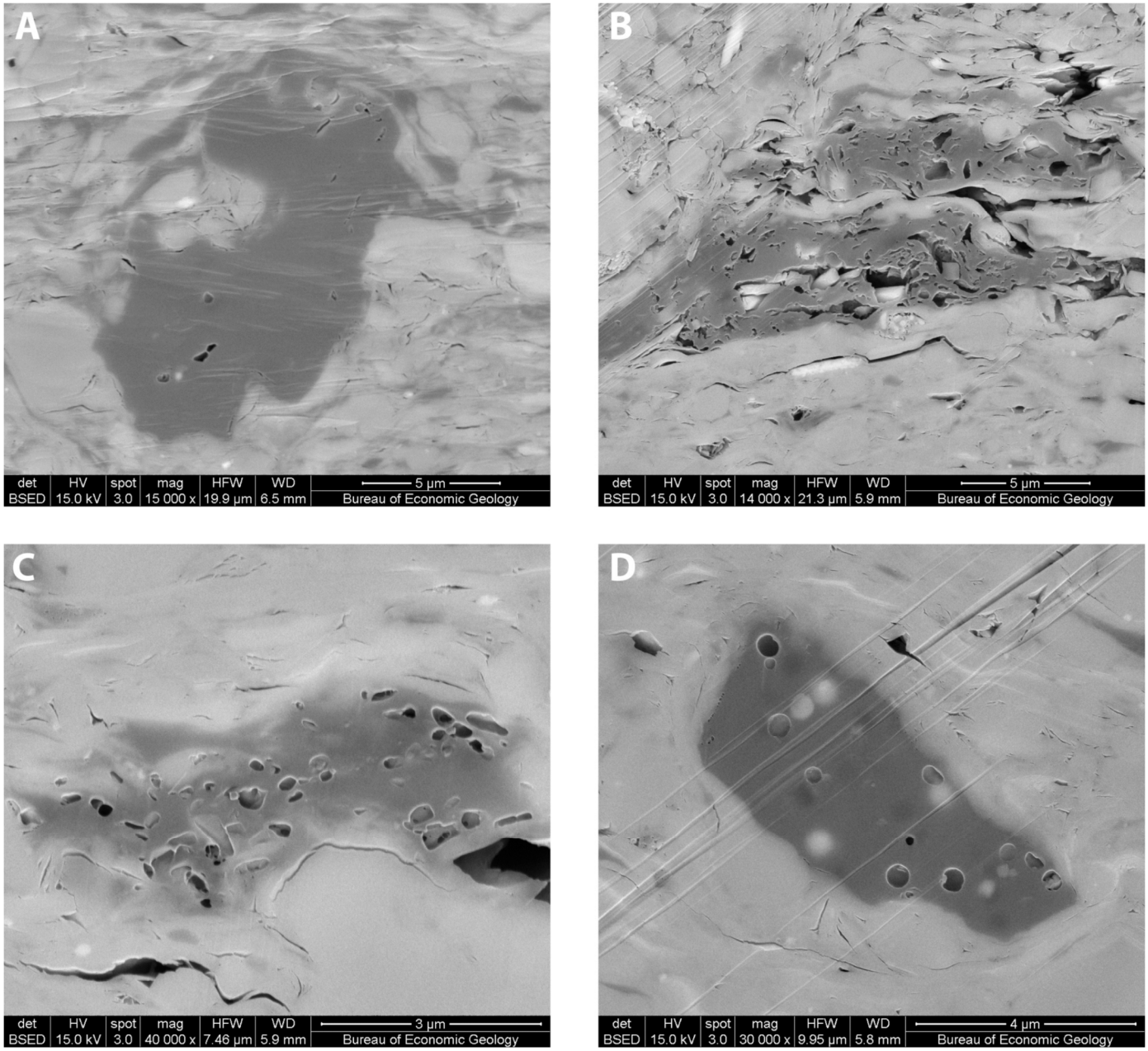

Figure 5. BSE images of organic-matter grains with pores, basal Eagle Ford Group. (A) Sparse pores in a large grain of organic matter. Sample from 4771 ft (1454.2 m). (B) Elongate pores in elongate organic-matter grains. Sample from 4774 ft (1455.1 m). (C) Rounded pores in an elongate organic-matter grain. Sample from 4774 ft (1455.1 m). (D) Sparse circular outline pores in an organic-matter grain. Sample from 4774 ft (1455.1 m).

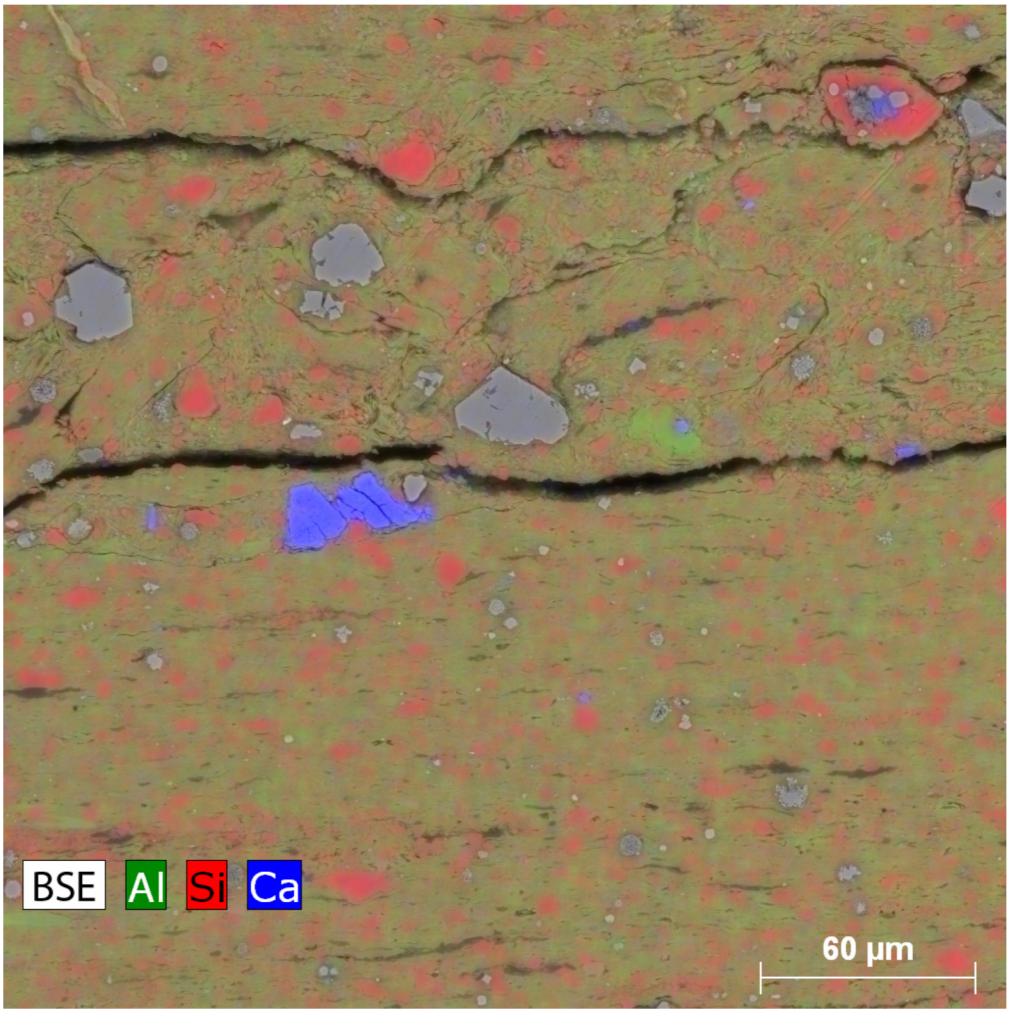

Figure 6. Combined color energy dispersive spectroscopy (EDS) maps superimposed on a BSE image. Sample is from a depth of 4774 ft (1455.1 m) at the base of the Eagle Ford Group. Red grains are quartz, green are clay minerals, and blue are calcite; most gray crystals are pyrite. Subhorizontal microfractures are unmineralized and interpreted to be artifacts.

from the breakdown of kerogen. It is thought that the organic-matter grains described here are kerogen, but evidence is not definitive.

In all three units, pores are found in silt- to sand-size organic-matter grains or composite grains rather than in the finer-grained matrix organic matter that is found in some samples. In the development of organic-matter pores at thermal maturities greater than 0.75% R_o, pores are more commonly found in matrix organic matter than in organic-matter grains. Where pores are present in organic-matter grains at high thermal maturity, the matrix organic matter typically also contains pores (Loucks et al., 2009). This difference is one argument for the pores in organic-matter grains at low thermal maturity being predepositional.

The Wilcox Group samples show no evidence of organic chemical reactions related to thermal maturation. The relatively large size of the organic-matter grains in these samples suggests they should be interpreted as kerogen, because pore space large enough to generate bitumen grains of this size is unlikely in these rocks. None of the organic matter present shows good textural evidence for being bitumen (Loucks and Reed, 2014; Milliken et al., 2014). Also, large numbers of interparticle pores are present in these samples, and the generation of bitumen tends to fill in such pores (e.g., Loucks and Reed, 2014). The diversity of pore types argues for either predepositional origin or development in heterogeneous varieties of kerogen.

Some Eagle Ford samples (4762.5 ft and 4771 ft [1451.6 m and 1454.2 m]) show evidence of organic chemical reactions related to thermal maturation. Migrated organic matter interpreted as bitumen is present in these samples despite the relatively low R_o of ~0.45%. Original intraparticle pore spaces in microfossils are filled with organic matter, presumably bitumen. Interparticle pores are also mostly filled with organic matter, some of which has a few micrometer-scale pores suggestive of partial bitumen filling of preexisting pores. The large elongate pores in some of the grains (Fig. 5B) are unlike the more spherical pores seen in organic matter from higher-thermal-maturity Eagle Ford samples (e.g., Pommer and Milliken, 2015; Schieber et al., 2016).

No definitive evidence has been seen in the Smithwick samples for the presence of bitumen. Slightly more deeply buried rocks of the Barnett Shale from the same cores do show some such evidence (Reed and Loucks, 2015). Given the thermal maturity of a few of the Smithwick samples (R_o of 0.71%), it is likely that some bitumen is also present in some of them. However, it is unlikely that the bitumen would form grain-size masses in these rocks given the difficulty of forming a silt-size pore in a mudrock at depth. Given the different pore texture present in the Smithwick samples than that seen in either the Eagle Ford or the Wilcox samples, the Smithwick pores could be syn- or postdepositional, and those of the other two units could be predepositional. The possible origins of the Smithwick pore texture will be discussed more fully in a later section.

Terrestrial Versus Marine Organic Matter

One of the best arguments for low-thermal-maturity porous organic matter being primarily terrestrial in origin is supplied by the Eagle Ford core examined in this study. In the bottommost layer of the unit (4774 ft [1455.1 m]), which has the fewest ma-

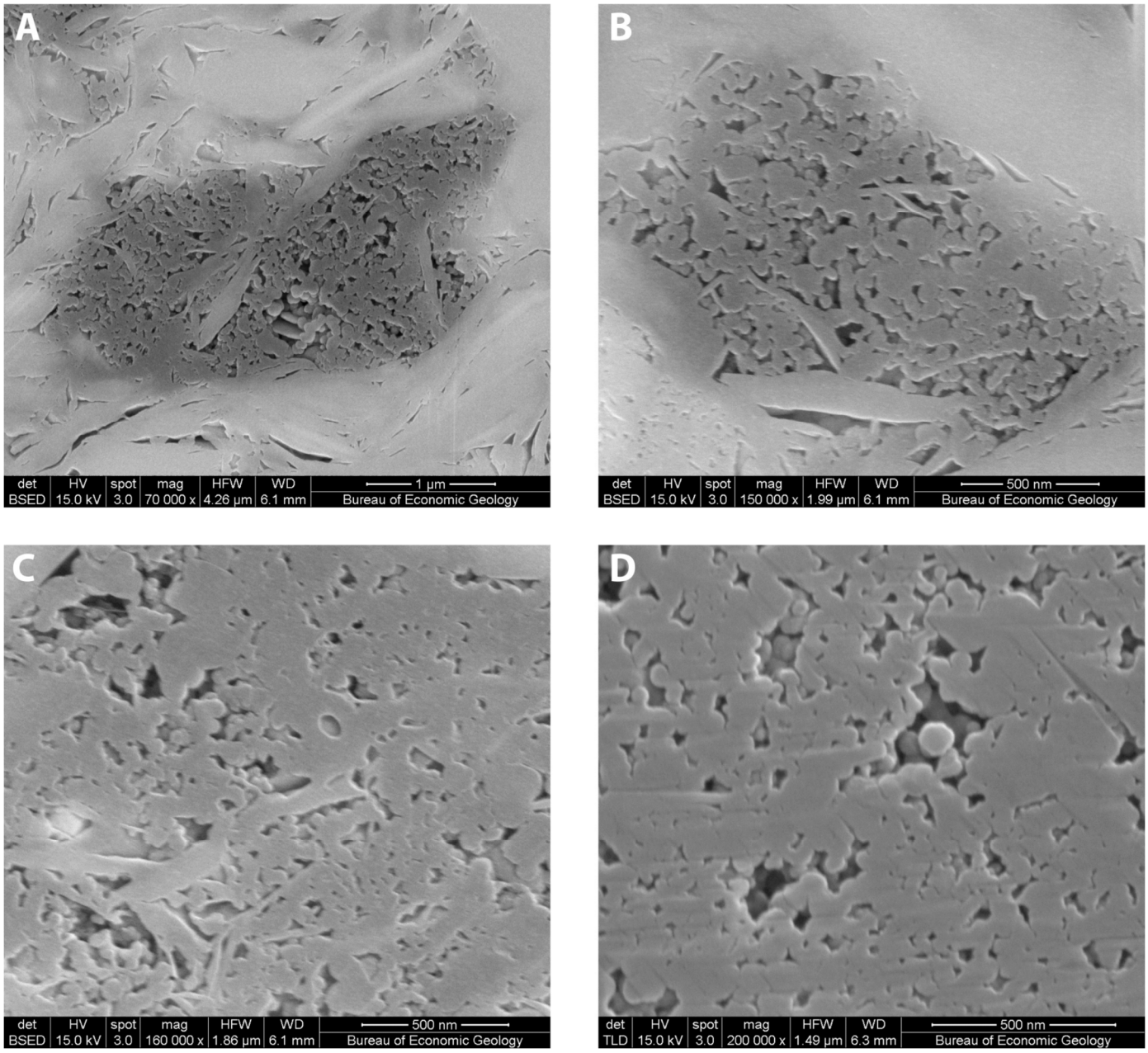

Figure 7. SEM images of porous organic-matter grains, Smithwick Shale. (A) BSE image of a porous organic-matter grain consisting of nanometer-scale spheres of organic matter and a few clay-mineral pieces. C. D. Scoggins A–2–1 well, 442 ft, McCulloch Co., calculated R_o of 0.53%. (B) BSE image of a porous organic-matter grain consisting of nanometer-scale spheres of organic matter and some clay minerals. C. D. Scoggins A–2–1 well, 442 ft (134.7 m), McCulloch Co., calculated R_o of 0.53%. (C) BSE image showing interior of a porous organic-matter grain consisting of nanometer-scale spheres. H. Johanson MC–1 well, 901 ft (274.6 m), McCulloch Co., calculated R_o of 0.65%. (D) Secondary electron image showing interior of a porous organic-matter grain. Organic-matter spheres that make up the grain are less distinct than those from shallower samples. J. A. Potter C–9–1 well, 1943.1 ft (592.3 m), Brown Co., calculated R_o of 0.67%.

rine characteristics and a type III kerogen geochemical signature, many of the organic-matter grains are porous. Moving upward to the layers containing marine microfossils but also significant vitrinite (4771 ft and 4762.5 ft [1451.6 m and 1454.2 m]), fewer organic-matter grains have pores. In the shallower samples from this core with very limited vitrinite, isolated pores are found in migrated organic matter thought to be bitumen, but not in organic-matter grains (Reed and Ruppel, 2012).

Pores in organic matter are not necessarily found in all terrestrial organic matter. Some studies of the Triassic Yanchang Shale from China (Loucks et al., 2017; Ko et al., 2017a; and references therein) have focused on pore systems. This unit is lacustrine in origin, and the studied rocks are at moderate thermal maturity (R_o ~0.9%). Loucks et al. (2017) delineated the organic-matter pores in this unit. Much of the organic matter is nonporous. What organic matter is porous has nanometer-scale pores, unlike the larger pores seen in terrestrial organic matter discussed in this study. Loucks et al. (2017) interpret the porous organic matter to be migrated bitumen. Organic matter they interpret to be type III kerogen (woody material) occurs in micrometer-size grains and has no pores.

Suggesting that some terrestrial organic matter has pores raises the issue of coals. Given that most coals are composed of terrestrial organic matter, there should be micrometer-scale and

smaller pores in coals. In many cases, there is—fusinite, semifusinite, and some other macerals (e.g., Papp et al., 1998) show predepositional pores. In a study similar to this one, Giffin et al. (2013) used broad-ion-beam milling and field-emission SEM to examine coal samples. They found few resolvable pores in vitrinite, but numerous pores in fusinite and other inertinite macerals.

Origin of Smithwick Shale Organic-Matter Texture

If present only in the Smithwick Shale, the organic-matter texture described here would be a mere curiosity. However, the rare presence of the texture in other units makes it more relevant, because it appears to be an indicator of an atypical organic-matter history.

Any proposed formation mechanism needs to account both for the formation of the spheres and their agglomeration into composite grains. Three different explanations for the particulate internal texture of organic-matter composite grains in the Smithwick have been considered. None of them, however, provide an entirely satisfactory explanation for why this texture would be so widespread in the Smithwick Shale but largely absent elsewhere.

First, nanoscale spheres in geologic samples have previously been reported (e.g., Folk, 1993) and have been termed "nannobacteria" by some workers. "Nannobacteria" are at best controversial (e.g., Velimirov, 2001; Raoult et al., 2008). This is mainly because the smallest confirmed living bacteria are ~200 nm in length (Luef et al., 2015), twice the size of the nanoscale spheres in the Smithwick. Nanoscale spheres of a corresponding diameter are common in some geologic samples (Folk, 1993) but are typically composed of calcite. Whatever process formed the basis for these spheres elsewhere may be operating in the Smithwick, as well, whether it is the proposed bacterial process or a complex chemical reaction (Raoult et al., 2008).

A second possibility is that the organic-matter texture results from biological activity, but by the formation of small pellets composed of even smaller spheres. The presence of some clay minerals within the organic-matter grains supports this possibility.

A third possibility is that the texture results from inhomogeneous conversion of kerogen to bitumen, perhaps influenced by preexisting heterogeneity in the kerogen. However, the apparent decrease in porosity with increasing thermal maturity seen in these samples (Fig. 7D) would argue against that situation, because more conversion would take place with increasing maturity.

In any case, the Smithwick organic matter behaves very differently than the slightly older marine organic matter in the Barnett Shale from the same area (Reed and Loucks, 2015). An examination of organic matter in the marine Marble Falls Limestone, which is partly contemporary with the Smithwick, would be useful.

CONCLUSIONS

Low-thermal-maturity organic matter can have pores in some units. This may be closely tied to a terrestrial origin for the organic matter.

The porous organic-matter grains present in the Wilcox and Eagle Ford samples are most likely predepositional in origin.

The porous organic matter present in the Smithwick Shale represents a type of organic-matter pore not previously described in the literature. The origin of this porous texture remains a matter for debate.

Before making definitive statements about the nature of organic-matter pores in a thermally mature organic matter, it is a good idea to have examined a corresponding low-thermal-maturity sample to see if it has porous organic matter.

ACKNOWLEDGMENTS

This research was funded by the Mudrock Systems Research Laboratory at the Bureau of Economic Geology, Jackson School of Geosciences, University of Texas at Austin. Sponsoring companies include: Anadarko, Apache, Aramco Services, BHP, BP, Cenovus, Centrica, Chesapeake, Cima, Cimarex, Chevron, Concho, ConocoPhillips, Cypress, Devon, Encana, ENI, EOG, EXCO, ExxonMobil, FEI, Geosun, Hess, Husky, IMP, Kerogen, Marathon, Murphy, Newfield, Oxy, Penn Virginia, Penn West, Pioneer, QEP, Repsol, Samson, Shell, Sinopec, StatOil, Talisman, Texas American Resources, The Unconventionals, University Lands, US EnerCorp, Valence, and YPF.

William Ambrose and Robert Loucks provided information and sampling suggestions for the Wilcox Group. James C. Hower provided access to unpublished vitrinite reflectance data from the Eagle Ford Group. Scott Hamlin provided insights into the stratigraphy and lithology of the Smithwick Formation. Stephen Ruppel suggested sampling of the basal Eagle Ford Group core. Lucy Ko reviewed an early draft of this manuscript. The Media Group at the Bureau of Economic Geology is thanked for graphics support. Joan Spaw, Tobi Kosanke, and an anonymous reviewer provided helpful comments. Technical editing at the Bureau of Economic Geology provided by Stephanie Jones.

Publication was authorized by the Director, Bureau of Economic Geology, Jackson School of Geosciences, University of Texas at Austin.

REFERENCES CITED

Breyer, J. A., ed., 2016, The Eagle Ford Shale: A renaissance in U.S. oil production: American Association of Petroleum Geologists Memoir 110, Tulsa, Oklahoma, 389 p., doi:10.1306/m1101306.

Bureau of Economic Geology, 1997, Tectonic map of Texas: Texas Bureau of Economic Geology, Austin, SM004, scale 1 in = 100 mi, 1 p.

Cardott, B. J., C. R. Landis, and M. E. Curtis, 2015, Post-oil solid bitumen network in the Woodford Shale, USA—A potential primary migration pathway: International Journal of Coal Geology, v. 139, p. 106–113, doi:10.1016/j.coal.2014.08.012.

Curtis, M. E., R. J. Ambrose, C. H. Sondergeld, and C. S. Rai, 2010, Structural characterization of gas shales on the micro- and nanoscales: Society of Petroleum Engineers Paper 137693, Richardson, Texas, 15 p., doi:10.2118/137693-MS.

Fisher, W. L., and J. McGowen, 1969, Depositional systems in Wilcox Group (Eocene) of Texas and their relation to occurrence of oil and gas: American Association of Petroleum Geologists Bulletin, v. 53, p. 30–54, doi:10.1306/5d25c591-16c1-11d7-8645000102c1865d.

Fishman, N. S., P. C. Hackley, H. A. Lowers, R. J. Hill, S. O. Egenhoff, D. D. Eberl, and A. E. Blum, 2012, The nature of porosity in organic-rich mudstones of the Upper Jurassic Kimmeridge Clay Formation, North Sea, offshore United Kingdom: International Journal of Coal Geology, v. 103, p. 32–50, doi:10.1016/j.coal.2012.07.012.

Folk, R. L., 1993, SEM imaging of bacteria and nannobacteria in carbonate sediments and rocks: Journal of Sedimentary Petrology, v. 63, p. 990–999, doi:10.1306/d4267c67-2b26-11d7-8648000102c1865d.

Giffin, S., R. Littke, J. Klaver, and J. L. Urai, 2013, Application of BIB–SEM technology to characterize macropore morphology in coal: International Journal of Coal Geology, v. 114, p. 85–95, doi:10.1016/j.coal.2013.02.009.

Harbor, R. L., 2011, Facies characterization and stratigraphic architecture of organic-rich mudrocks, Upper Cretaceous Eagle Ford Formation, South Texas: M.S. Thesis, University of Texas at Austin, 184 p.

Hentz, T. F., W. A. Ambrose, and D. C. Smith, 2014, Eaglebine play of the southwestern East Texas Basin: Stratigraphic and deposi-

tional framework of the Upper Cretaceous (Cenomanian-Turonian) Woodbine and Eagle Ford: American Association of Petroleum Geologists Bulletin, v. 98, p. 2551–2580, doi:10.1306/07071413232.

Hughes, N., and Rowe, H. D., 2010, Chemostratigraphy and paleodepositional conditions of the Pennsylvanian Smithwick Formation, Fort Worth Basin, Texas (abs.): Geological Society of America Abstracts with Programs, v. 42, no. 5, p. 298.

Jarvie, D. M., B. L. Claxton, F. Henk, and J. T. Breyer, 2001, Oil and shale gas from the Barnett Shale, Fort Worth Basin, Texas (abs.): American Association of Petroleum Geologists Annual Meeting Program, v. 10, p. A100, doi:10.1306/8626e28d-173b-11d7-8645000102c1865d. Available also at American Association of Petroleum Geologists Search and Discovery Article 90906, Tulsa, Oklahoma, 1 p., <http://www.searchanddiscovery.com/abstracts/html/2001/annual/abstracts/0386.htm> Last accessed September 13, 2017.

Kier, R. S., L. F. Brown, Jr., and E. F. McBride, 1980, The Mississippian and Pennsylvanian (Carboniferous) systems in the United States—Texas: U.S. Geological Survey Professional Paper 1110–S, 45 p., <https://pubs.usgs.gov/pp/1110a-l/report.pdf> Last accessed September 13, 2017.

Klaver, J., G. Desbois, J. L. Urai, and R. Littke, 2012, BIB–SEM study of the pore space morphology in early mature Posidonia Shale from the Hils area, Germany: International Journal of Coal Geology, v. 103, p. 12–25, doi:10.1016/j.coal.2012.06.012.

Klaver, J., G. Desbois, R. Litke, and J. L. Urai, 2015, BIB–SEM characterization of pore space morphology and distribution in postmature to overmature samples from the Haynesville and Bossier shales: Marine and Petroleum Geology, v. 59, p. 451–466, doi:10.1016/j.marpetgeo.2014.09.020.

Ko, L. T., R. G. Loucks, K. L. Milliken, Q. Liang, T. Zhang, X. Sun, P. C. Hackley, S. C. Ruppel, and S. Peng, 2017a, Controls on pore types and pore-size distribution in the Upper Triassic Yanchang Formation, Ordos Basin, China: Implications for pore-evolution models of lacustrine mudrocks: Interpretation, v. 5, no. 2, p. 127–148, doi:10.1190/int-2016-0115.1.

Ko, L. T., R. G. Loucks, S. C. Ruppel, T. Zhang, and S. Peng, 2017b, Origin and characterization of Eagle Ford pore networks in the South Texas Upper Cretaceous Shelf: American Association of Petroleum Geologists Bulletin, v. 101, p. 387–418, doi:10.1306/08051616035.

Loucks, R. G., and R. M. Reed, 2014, Scanning-electron-microscope petrographic evidence for distinguishing organic-matter pores associated with depositional organic matter versus migrated organic matter in mudrocks: Gulf Coast Association of Geological Societies Journal, v. 3, p. 51–60, <http://www.gcags.org/Journal/2014.GCAGS.Journal/GCAGS.Journal.2014.vol3.p51-60.Loucks.and.Reed.pdf> Last accessed September 13, 2017.

Loucks, R. G., R. M. Reed, S. C. Ruppel, and U. Hammes, 2012, Spectrum of pore types and networks in mudrocks and a descriptive classification for matrix-related mudrock pores: American Association of Petroleum Geologists Bulletin, v. 96, p. 1071–1098, doi:10.1306/08171111061.

Loucks, R. G., R. M. Reed, S. C. Ruppel, and D. M. Jarvie, 2009, Morphology, genesis, and distribution of nanometer-scale pores in siliceous mudstones of the Mississippian Barnett Shale: Journal of Sedimentary Research, v. 79, p. 848–861, doi:10.2110/jsr.2009.092.

Loucks, R. G., S. C. Ruppel, X. Wang, L. Ko, S. Peng, T. Zhang, H. D. Rowe, and P. Smith, 2017, Pore types, pore-network analysis, and pore quantification of the lacustrine shale-hydrocarbon system in the Late Triassic Yanchang Formation in the southeastern Ordos Basin, China: Interpretation, v. 5, no. 2, p. 1–17, doi:10.1190/INT-2016-0094.1.

Luef, B., K. R. Frischkorn, K. C. Wrighton, H.–Y. N. Holman, G. Birarda, B. C. Thomas, A. Singh, K. H. Williams, C. E. Siegerist, S. G. Tringe, K. H. Downing, L. R. Comolli, and J. F. Banfield, 2015, Diverse uncultivated ultra-small bacterial cells in groundwater: Nature Communications, v. 6, no. 6372, 8 p., doi:10.1038/ncomms7372.

Milliken, K. L., L. T. Ko, M. Pommer, and K. M. Marsaglia, 2014, SEM petrography of eastern Mediterranean sapropels: Analogue data for assessing organic matter in oil and gas shales: Journal of Sedimentary Research, v. 84, p. 961–974, doi:10.2110/jsr.2014.75.

Milliken, K. L., M. Rudnicki, D. N. Awwiller, and T. Zhang, 2013, Organic matter-hosted pore system, Marcellus Formation (Devonian), Pennsylvania, USA: American Association of Petroleum Geologists, Bulletin, v. 97, p. 177–200, doi:10.1306/07231212048.

Mukhopadhyay, P. K., 1989, Organic petrography and organic geochemistry of Texas Tertiary coals in relation to depositional environment and hydrocarbon generation: Texas Bureau of Economic Geology Report of Investigations 188, Austin, 118 p., doi:10.23867/ri0188d.

Papp, A. P., J. C. Hower, and D. C. Peters, eds., 1998, Atlas of coal geology: American Association of Petroleum Geologists Studies in Geology 45, Tulsa, Oklahoma, CD–ROM, doi:10.1306/St45CD655.

Pollastro, R. M., D. M. Jarvie, R. J. Hill, and C. W. Adams, 2007, Geologic framework of the Mississippian Barnett Shale, Barnett-Paleozoic total petroleum system, Bend Arch–Fort Worth Basin, Texas: American Association of Petroleum Geologists Bulletin, v. 91, p. 405–436, doi:10.1306/10300606008.

Pommer, M., and K. L. Milliken, 2015, Pore types and pore-size distributions across thermal maturity, Eagle Ford Formation, southern Texas: American Association of Petroleum Geologists Bulletin, v. 99, p. 1713–1744, doi:10.1306/03051514151.

Raoult, D., M. Drancourt, S. Azza, C. Nappez, R. Guieu, J.–M. Rolain, P. Fourquet, B. Campagna, B. La Scola, J.–L. Mege, P. Mansuelle, E. Lechevalier, Y. Berland, J.–P. Gorvel, and P. Renesto, 2008, Nanobacteria are mineralo fetuin complexes: PLoS Pathogens, v. 4, no. 2, e41, 8 p., doi:10.1371/journal.ppat.0040041.

Reed, R. M., and R. G. Loucks, 2015, Low-thermal-maturity (<0.7% VR) mudrock pore systems: Mississippian Barnett Shale, southern Fort Worth Basin: Gulf Coast Association of Geological Societies Journal, v. 4, p. 15–28, <http://www.gcags.org/Journal/2015.GCAGS.Journal/2015.Journal.v4.2.p15-28.Reed.and.Loucks.press.pdf> Last accessed September 13, 2017.

Reed, R. M., R. G. Loucks, and L. T. Ko, 2017, Pores observed in organic matter in mudrocks: A ten-year retrospective (abs.): American Association of Petroleum Geologists Search and Discovery Article 90291, Tulsa, Oklahoma, 1 p. <http://www.searchanddiscovery.com/abstracts/html/2017/90291ace/abstracts/2605375.html> Last accessed September 13, 2017.

Reed, R. M., and S. C. Ruppel, 2012, Pore morphology and distribution in the Cretaceous Eagle Ford Shale, South Texas, USA: Gulf Coast Association of Geological Societies Transactions, v. 62, p. 599–603.

Roduit, N., 2008, JMICROVISION version 1.2.7: Image analysis toolbox for measuring and quantifying components of high-definition images, <http://www.jmicrovision.com> Accessed March 13, 2017.

Schieber, J., 1996, Early diagenetic silica deposition in algal cysts and spores: A source of sand in black shales?: Journal of Sedimentary Research, v. 66, p. 175–183, doi:10.1306/d42682ed-2b26-11d7-8648000102c1865d.

Schieber, J., 2010. Common themes in the formation and preservation of intrinsic porosity in shales and mudstones—Illustrated with examples across the Phanerozoic: Society of Petroleum Engineers Paper SPE–132370, Richardson, Texas, 10 p., doi:10.2118/132370-m.

Schieber, J., R. Lazar, K. Bohacs, B. Klimentidis, J. Ottmann, and M. Dumitrescu, 2016, An SEM study of porosity in the Eagle Ford Shale of Texas—Pore types and porosity distribution in a depositional and sequence stratigraphic context, *in* J. A. Breyer, ed., The Eagle Ford Shale: A renaissance in U.S. oil production: American Association of Petroleum

Geologists Memoir 110, Tulsa, Oklahoma, p. 167–186, doi:10.1306/13541961m1103589.
Velimirov, B., 2001, Nanobacteria, ultramicrobacteria and starvation forms: A search for the smallest metabolizing bacterium: Microbes and Environments, v. 16, no. 2, p. 67–77, doi:10.1264/jsme2.2001.67.